RESEARCH

The therapeutic efficacy comparison of MSCs derived different tissues unveilings anti-apoptosis more crucial than angiogenesis in treating acute myocardial infarction

Mingjie Pan[1†], Yueyue Xu[2†], Yaping Wang[3], Yue Jiang[4], Yuanyuan Xie[4], Chenxu Tai[4], Wenqing Wang[4] and Bin Wang[3,4*]

Abstract

Background Myocardial infarction (MI) is a severe disease that often associated with impaired angiogenesis and increased myocardial apoptosis. Mesenchymal stromal cells (MSCs) have been a promising candidate for treating myocardial infarction. However, functional heterogeneity of MSCs leads to inconsistent therapeutic efficiency and the current MSCs-based therapy lacks the concept and implementation of precision medicine. In this study, we compared the cardioprotective effect of UCMSCs and ADMSCs targeting the angiogenesis in a mouse MI model and screened out optimum MSCs candidate for precise clinical application.

Methods The gene expression profiles of UCMSCs and ADMSCs were investigated through RNA sequencing analysis. To compare their angiogenic potential, we performed tube formation assay, Matrigel plug assays, and aortic ring assay, and analyzed pro-angiogenic genes via qPCR. Subsequently, UCMSCs and ADMSCs were respectively injected into myocardium after MI surgery in mice. On day 28 post-MI, echocardiography was performed to assess cardiac function. Histological analysis was performed to assess MSCs retention, angiogenesis, and myocardial apoptosis. Additionally, the anti-apoptosis effects mediated by MSCs were further evaluated using flow cytometry in hypoxia H9C2 and HL-1 cells.

Results The RNA sequencing analysis revealed differences in gene expression related to angiogenesis and apoptosis pathways between UCMSCs and ADMSCs. UCMSCs presented greater pro-angiogenesis activity than ADMSCs in vitro and in vivo. Both of UCMSCs and ADMSCs improved cardiac function, decreased infarction area and inhibited cardiomyocyte apoptosis while promoting angiogenesis post-MI in mice. Notably, ADMSCs exerted a better cardioprotective function than UCMSCs and stronger anti-apoptotic effect on residual cardiomyocytes.

---

†Mingjie Pan and Yueyue Xu contributed equally to this work.

*Correspondence:
Bin Wang
wangbin022800@126.com

Full list of author information is available at the end of the article

Conclusions The protection of residual cells survival played a more prominent role than angiogenesis in MSCs-based therapy for acute MI. Our study provides new insights into therapeutic strategies and suggests that the optimal type of MSCs can be screened based on their tissue heterogeneity for precise clinical applications in acute MI.

Keywords Myocardial infarction, MSCs, Heterogeneity, Angiogenesis, Apoptosis

Introduction

Myocardial infarction (MI) is a leading cause of death worldwide caused by the occlusion of blood flow in the cardiac coronary arteries. Restricted blood supply causes irreversible loss of cardiomyocytes, which eventually leads to severely impaired cardiac function, resulting in a significant decrease in quality of life, and increased mortality. Myocardial repair and regeneration has always been a heated and difficult topic in medical research. After a heart attack, a complex series of repair and regeneration processes are triggered to restore myocardial function, involving inflammatory responses, apoptosis and angiogenesis. Among them, angiogenesis is the pivotal process of myocardial repair after myocardial injury, which is crucial for restoring blood supply and promoting the survival and regeneration of cardiomyocytes [1–4].

Cardiomyocytes will be necrotic due to ischemia and hypoxia, which results from interrupted or reduced blood flow within the heart caused by a blockage in the coronary artery. The formation of new blood vessels facilitates the survival and regeneration of cardiomyocytes following ischemic injury by conferring better perfusion to the myocardium. Neovascularization is a process of developing new vascular networks, primarily mediated by the proliferation, migration, and differentiation of vascular endothelial cells (ECs), which is augmented by various growth factors, cytokines and hormones, such as vascular endothelial growth factor (VEGF) and basic fibroblast growth factor (bFGF). Therefore, angiogenesis is vital for promoting reperfusion and functional recovery of ischemic heart and the induction of cardiac angiogenesis has become one of the key strategies in MI treatment [5–6].

At present, the routine treatments for MI include medications and surgeries, such as aspirin enteric-coated tablets, clopidogrel hydrogen sulfate tablets and percutaneous coronary intervention (PCI), which possesses a certain degree of efficacy in promoting angiogenesis and enhancing the survival of cardiac cells, thereby conducive to the recovery of cardiac function [7]. In addition, stem cells are emerging as a potential therapy for MI [8].

Mesenchymal stromal cells (MSCs), a type of adult stem cells isolated from multiple tissues including bone marrow, adipose tissue, umbilical cord, and many other locations, are considered ideal candidates for cardiac repair and regeneration due to their remarkable properties such as self-renewal, multipotent differentiation, minimal immunogenicity, strong immunomodulatory effects, and, most importantly, their capability to differentiate into smooth muscle cells (SMCs), ECs, cardiomyocytes, and others [9–11]. Indeed, the injection of MSCs has achieved desired therapeutic effects in post-MI treatment in clinical trials, as evidenced by improved cardiac performance, enhanced quality of life, as well as reduced readmission rates and mortality in patients with MI [12–16].

Although MSCs can alleviate myocardial ischemic injury and improve cardiac function. MSCs exhibited substantial heterogeneity depending on their tissue origin not only in biological properties such as differentiation potential, immunomodulatory capacity and migratory ability, but also in morphological characteristics, and gene expression profiles, In addition to tissue heterogeneity, MSCs from the same tissue types of different donors differ considerably. The prevalent use of readily accessible cell sources and non-standardized culture conditions in current preclinical studies, as well as the unoptimized timing, route, and dose for MSCs delivery [17–19], significantly compromises the comparability of experimental results. Consequently, the heterogeneity may be a crucial factor affecting the therapeutic outcomes of MSCs in specific clinical applications, as evidenced by numerous recent studies [20–24]. Similarly, it has been reported that the therapeutic effects of MSCs in MI or osteoarthritis can be significantly reinforced due to reduced heterogeneity, improved differentiation potential and enhanced immunomodulatory function through optimized isolation, culture conditions, and pretreatment approaches for MSCs [25–27].

Given the critical role of pro-angiogenesis in cardiac repair and regeneration after MI, recent studies have primarly focused on the pro-angiogenic potential of MSCs and their paracrine factors, such as VEGF, bFGF, and hepatocyte growth factor (HGF) in myocardial infarction treatment. In this study, we compared clinical-grade MSCs from different tissue sources, umbilical cord-derived MSCs (UCMSCs) and adipose-derived MSCs (ADMSCs), in terms of their angiogenic potential. We further explored whether their differences in angiogenic capacity translate to varied accuracy and effectiveness in MI therapy, and thus optimized the treatment regimen and augmented the therapeutic outcomes for future clinical applications.

Methods

The work has been reported in line with the ARRIVE guidelines 2.0.

Pan *et al. Stem Cell Research & Therapy*   (2025) 16:236

Page 3 of 15

MSCs cell culture and identification

Donor screening was strictly performed before sampling. The screening includes a physical examination, detailed medical history review, and infectious disease testing. The general characteristics of the donors are detailed in Table S1.

The clinical-grade UCMSCs and ADMSCs employed in this study were greatly optimized and complied with GMP quality standards mentioned in our previous research, including isolation, cultivation, identification, quality control, and storage [23]. The MSCs were cultured in DMEM medium supplemented with 10%FBS (Gibco, USA) and at 37℃ in an incubator with 5% CO2. The UCMSCs used in this study were derived from three donors, and ADMSCs were obtained from three separate donors, resulting in a total of six MSCs lines for transcriptome sequencing analysis. To minimize inter-donor variability, UCMSCs and ADMSCs were each mixed at a 1:1:1 ratio from three separate donors. Detailed descriptions were listed in Table S2.

Flow cytometry (Accuri C6 Plus, BD) was used to determine the surface marker expressions of UCMSCs and ADMSCs, including CD14, CD19, CD34, CD45, CD73, CD90, CD105, and HLA-DR (BD, USA), with isotype-matched antibody as negative control. Data were analyzed using Flow Jo V10 software. In addition, the differentiation potential of UCMSCs and ADMSCs into adipogenesis and osteogenesis was evaluated after culturing them in differentiation medium (Gibco, USA), according to our previous research [23, 28, 29].

Transcriptome sequencing analysis between UCMSCs and ADMSCs

OE Biotech Co., Ltd. (Shanghai, China) conducted RNA extraction, processing, libraries construction and transcriptome sequencing and analysis. DESeq R package was used for differential gene expression analyses. The screening criteria for differentially expressed genes (DEGs) were p value < 0.05 and fold change > 2 or fold change < 0.5. Heatmap and KEGG enrichment analysis of DEGs were extracted from the analysis. Employing ssGSEA in GSVA (version 1.44.5), genes in the highlighted pathway was used to calculate pathway scores, to characterize the difference of function between UCMSCs and ADMSCs [30].

Endothelial cell tube formation assay

The pro-angiogenic potential of conditioned medium from UCMSCs and ADMSCs was assessed in vitro. First, UCMSCs and ADMSCs were incubated in DMEM medium supplemented with 1%FBS. Their conditioned medium was then collected and centrifuged at 2000× g for 10 min at 4 °C to remove dead cells and cell debris. Next, human umbilical vein endothelial cells (HUVECs) diluted with conditioned medium collected from UCMSCs and ADMSCs, respectively, were seeded at a density of 20,000 cells/well in a 96-well plate coated with Matrigel 1 h before at 37 °C (50μL/well) (BD, USA). After 8 h of incubation, capillary-like tube formation was randomly photographed, and the total tube length, number of nodes, and number of junctions were calculated by ImageJ software (USA).

Animals

Female BALB/C nude mice aged 6 to 8 weeks and male C57BL/6 mice aged 7 to 8 weeks were used for Matrigel plug assay and MI model, respectively (Gem Pharmatech Co., Ltd., China). All animal experiments were performed in compliance with the guidelines and regulations of the Animal Experimentation Committee of Nanjing Medical University (Ethics Committee of Nanjing First Hospital; Approval No. DWSY-22115244). The mice were raised in the experimental animal center (temperature at 23 ± 2 °C, and air humidity at 40–60%), with room kept dark for 12 h and illuminating for 12 h.

Matrigel plug assay

Briefly, mice were anesthetized with 1.0-1.5% isoflurane(RWD, R510-22-10, China). A total of 5×10^5 UCMSCs or ADMSCs were mixed with Liquid Matrigel (BD, USA), stored at 4 °C, and injected subcutaneously (200ul/site, 2 sites/mouse) into the left and right groin of female BALB/C nude mice. Matrigel alone was used as negative control.

On day 14 after injection, the mice were placed in a CO_2 euthanasia chamber (YUYAN INSTRUMENTS, China) with a CO_2 flow rate at 2 L/min, lasting for 3–5 min until the mice were fully euthanized. The Matrigel plugs were then harvested and immediately embedded in optimal cutting temperature compound (OCT) (Leica, Germany) for freezing. The plugs were subsequently sliced into to 5 μm sections. Neovasculature was assessed using anti-mouse CD31 (BD, USA) for immunofluorescence staining.

Conditioned medium collection from UCMSCs and ADMSCs

UCMSCs and ADMSCs were cultured to 70–80% confluence in 6-well plates. After replacing the medium with serum-free DMEM medium and incubating for 24 h, conditioned medium was collected, centrifuged (2000 × g, 30 min), aliquoted, and stored at – 80 °C. Cells were lysed in RIPA buffer with protease/phosphatase inhibitors, homogenized, and the total protein concentration was determined using a BCA assay (Beyotime, China) for subsequent normalization of the conditioned medium.

Ex vivo aortic ring sprouting assay

To further evaluate the angiogenic properties of UCMSCs and ADMSCs, the ex vivo mouse aortic ring assay was performed according to previous report [31]. Thoracic aortas were dissected from 11week-old male C57BL/6 mice (Gem Pharmatech Co., Ltd., China). Aortas were cut into rings (0.5–1 mm long) and then incubated in DMEM (Gibco, USA) supplemented with 1% penicillin/streptomycin in a dish overnight at $37℃/5\%$ CO2. Next day, rat tail-derived type I collagen (Millipore, USA) was transferred to the 96-well plates (50μL/well). Then, the rings randomly placed and embedded in type I collagen (one ring per well) and incubated at 37 °C/5% CO2 for 1 h. Subsequently, 150 μl of conditioned medium from UCMSCs and ADMSCs supplemented with 2.5% FBS were added to each well. The rings cultured with DMEM medium supplemented with 2.5% FBS as control. The culture medium was changed every other day. Rings were imaged with an microscope on day 10. The rings were photographed and the number of angiogenic sprouting was counted.

RNA extraction and qRT-PCR

qRT-PCR was performed to analyze the expression of four major pro-angiogenic growth factors, bFGF, epidermal growth factor (EGF), HGF, VEGF and the cardioprotective factors insulin-like Growth Factor-1(IGF-1). Total RNA was extracted from UCMSCs or ADMSCs with TRIzol reagent (Vazyme, China). cDNA was synthesized using the Hiscript III reverse transcriptase (Vazyme, China). PCR was performed with the SYBR Green Real-Time PCR Master Mix Kit (Vazyme, China) according to the manufacturer's instructions. All quantitative PCR primers were synthesized by Sangon Biotech (China) and listed in Table S3. Data were normalized to GAPDH.

Establishing model of myocardium infarction and MSCs administration

The myocardial infarction model was established in male C57BL/6 mice by ligation of the left anterior descending coronary artery (LAD). Briefly, the mice were anesthetized using 2% isoflurane with an animal ventilator at 120 breaths/min for assisted ventilation, and maintained under continuous inhalation of 1.0-1.5% isoflurane during the surgery. A thoracotomy was performed to expose the heart, and the left anterior descending coronary artery was ligated with a 7–0 silk suture midway between the left atrium and the apex of the heart. Successful occlusion of coronary artery was confirmed by the myocardium distal to the coronary ligation turning white immediately.

After establishment of the MI model, the mice were randomly divided into four groups: (1) sham group ($n = 5$), the LAD was not ligated; (2) MI group ($n = 8$),

received myocardial injection of saline (40 μL); (3) MSCs treatment groups ($n = 8$ per group), UCMSCs and ADMSCs, a total of 2.5×10^5 fifth-passage cells, based on previous research, were suspended in 40 μl saline and injected at three sites in the border zone immediately after LAD ligation (within 5 min) [32]. After surgery, mice were carefully transferred to a heating pad at 35–37 °C for natural awakening. Collection of hearts was initiated immediately for further study following mice enthanasia mentioned above.

Echocardiography

Transthoracic echocardiography was performed to evaluate cardiac function (VisualSonics, Canada) on day 28 post-MI. After the mice were anesthetized with 1.0–1.5% isoflurane, two-dimensional M-model images were acquired and the left ventricular ejection fraction (LVEF) and left ventricular fractional shortening (LVFS) were recorded.

Histological analysis

Hearts were collected from the different groups on day 28 post-MI, fixed in 4% paraformaldehyde, embedded in paraffin, or embedded in OCT and sectioned into 5 μm slices. Masson's trichrome staining (Solarbio, China) was performed to assess scar size according to the manufacturer's recommendations. Briefly, the myocardial tissue above the ligation site of the left anterior descending coronary artery (LAD) was carefully excised. Tissue sections (5 μm thick) were obtained approximately 1 mm below the ligation site, perpendicular to the left ventricular long axis. The sections were stained with Masson's trichrome, and the average ratio of the fibrotic area to the total left ventricular (LV) cross-sectional area (scar area/LV%) was quantified using ImageJ software.

Immunofluorescence analysis

For quantification of capillary density on day 28 after MSCs transplantation in paraffin or frozen sections. After hydration and retrieval with antigens in paraffin sections or frozen sections fixed with paraformaldehyde for 30 min. All sections were permeabilized with PBS containing 0.5% Triton X-100 (Beyotime, China) for 10 min. Next, the sections were blocked with 5% bovine serum albumin (BSA) (Biosharp, China) for 1 h and incubated with primary antibodies including CD31 and α-SMA (Abcam, UK) at 4 °C overnight, followed by incubation with goat anti-rabbit IgG second antibody conjugated to Alexa Fluor 568 (Invitrogen, USA) for 1 h at room temperature. Subsequently, cell nuclei were stained with DAPI (Abcam, UK). Microscopic pictures were captured under a confocal microscope (Leica, Germany).

Delivery of CM-DiI-labeled MSCs into infarcted myocardium

UCMSCs and ADMSCs were labeled with Cell Tracker™ CM-DiI (CM-DiI, invitrogen, USA) according to the manufacturer's guidance. In brief, MSCs were digested and incubated with a CM-DiI solution at a concentration of 20 μg/mL at 37 ℃ for 15 min, followed by incubation at 4 ℃ for another 15 min. The CM-DiI-labeled MSCs were directly delivered into the border zones of the infarcted myocardium in mice following MI surgery. After cell transplantation, the hearts of the mice were collected on day 7 and day 14 and frozen sections were prepared. The distribution of labeled cells (red) in the hearts was observed under a fluorescence microscope (Leica, Germany) to evaluate the retention of MSCs.

TUNEL staining

Apoptosis of cardiomyocytes was evaluated by terminal deoxynucleotidyl transferase dUTP nick end labeling staining (TUNEL), a sensitive index for evaluating apoptosis. Frozen sections of mouse hearts collected on day 1 and day 7 after MSCs transplantation were detected by TUNEL staining assay (Vazyme, China) to quantify the myocardial apoptosis. Briefly, the heart sections were fixed in 4% paraformaldehyde and permeabilized with 0.5% Triton X-100. The sections were then blocked with 5% BSA for 1 h at room temperature and incubated in the TUNEL reaction mixture at 37° C for 1 h. Subsequently, the sections were incubated with a primary polyclonal rabbit anti-cTnT (Abcam, UK), followed by a secondary goat anti-rabbit IgG antibodies conjugated with Alexa Fluor 488 (Invitrogen, USA). Nuclei were counterstained with DAPI (Abcam, UK). Images were acquired using a confocal microscope (Leica, Germany). The number of TUNEL-positive cells was represented as the ratio of apoptotic nuclei to total nuclei.

Western blotting of myocardial tissue

Myocardial tissues were transferred from liquid nitrogen to room temperature and lysed with RIPA lysis buffer and the total protein concentration was quantified using a BCA protein assay, as mentioned above. Protein samples were separated by SDS-PAGE and transferred to PVDF membranes (Millipore, USA). After blocking the membranes with 5% BSA for 1 h, primary antibodies were applied and incubated at 4 ℃ overnight. The following day, the secondary antibody (Beyotime, China) was applied for 1 h at room temperature. The primary antibodies were anti-GAPDH (ABclonal, China), anti-Bax (Beyotime, China), anti-Caspase-3 (CST, USA), respectively. Protein bands on the membranes were visualized using an enhanced chemiluminescence kit (Vazyme, China).

H9C2 and HL-1 cells apoptosis under hypoxic conditions

The rat cardiomyoblasts (H9C2 cells) and mouse atrial cardiomyocytes (HL-1 cells) were obtained from the Department of Thoracic and Cardiovascular Surgery, Nanjing First Hospital (Nanjing, China). The cells were cultured in DMEM-high glucose (Gibco, USA) containing 10% FBS and 1% penicillin at 37 ℃ with 5% CO2. When UCMSCs and ADMSCs cultured in T75 flasks reached 80-90% confluence, they were washed three times with PBS and replaced by serum- and glucose-free medium (Gibco, USA) for 24 h. Subsequently, H9C2 and HL-1 cells were cultured in the serum- and glucose-free conditioned medium collected from UCMSCs and ADMSCs for 8 h, and H9C2 and HL-1 cells were then transferred to a hypoxic chamber (MGC, Japan) for 3 h to mimic the myocardial hypoxia injury in vitro. Each experiment was repeated three times.

Assessment of apoptosis with flow cytometry

Double staining with fluorescein isothiocyanate (FITC)-conjugated Annexin V and propidium iodide (PI) was used to identify apoptotic cells (KeyGEN, China). H9C2 and HL-1 cells, along with their culture supernatant, were harvested and washed with PBS, then resuspened in binding buffer. FITC-Annexin V and PI were added, and cells were incubated in the dark for 15 min at room temperature. Finally, cellular fluorescence was detected by flow cytometry, respectively (Accuri C6 Plus, BD, Cyto-flexS, BECKMAN), and the data were analyzed using FlowJo software.

Statistical analysis

All values were presented as mean ± standard derivation (SD). A one-way ANOVA was used for comparisons involving more than two groups. t-tests was used for comparisons between two groups. GraphPad prism version 8.0 (GraphPad Software, USA) was used to estimate statistical significance and generate graphs. $p < 0.05$ indicated the difference was of statistical significance.

Results

Gene expression heterogeneity of UCMSCs and ADMSCs

In the present study, UCMSCs and ADMSCs had similar identification profiles, including strong expression of positive surface markers of CD105, CD90, and CD73 (over 95% percentage) and negative expression of CD14, CD34, CD45, CD19, and HLA-DR (less than 2% percentage) (Fig. 1A). The quantitative analysis results of surface markers are listed in Table S4. In addition, both UCMSCs and ADMSCs showed a multiple differentiation potential towards adipogenesis and osteogenesis (Fig. 1B). To investigate the tissue heterogeneities of UCMSCs and ADMSCs (three donors for each type of MSCs), RNA-sequence analysis was performed, revealing 2776
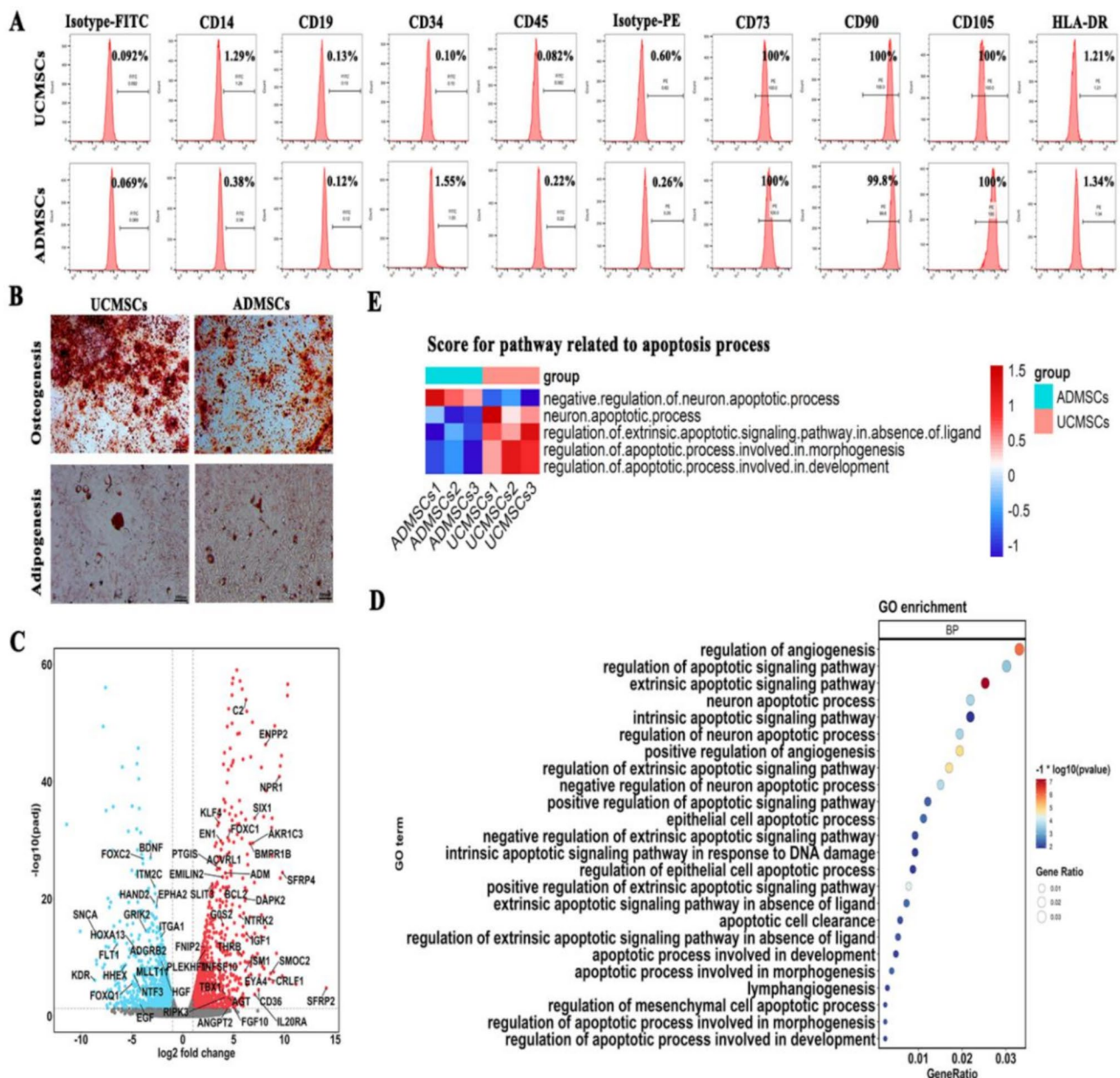
Fig. 1 Tissue heterogeneity of UCMSCs and ADMSCs. (**A**) Surface marker analysis of UCMSCs and ADMSCs by flow cytometry. (**B**) Adipogenic andOs-teogenetic differentiation potentials of UCMSCs and ADMSCs using Oil Red O staining and Alizarin Red staining, respectively. (**C**) Volcano plot displaying up- and down-regulated genes in UCMSCs and ADMSCs. Top DEGs that have been reported to be associated with angiogenesis and anti-apoptosis are labeled in the figure. (**D**) Bubble plot analysis showing the GO enrichment analysis of angiogenesis-related and apoptotic-related significant pathways of DEGs between UCMSCs and ADMSCs. three donors/each kind MSCs. (**E**) Heatmap of score showed the function level of apoptotic-related pathways between UCMSCs and ADMSCs. The color of each square indicates the scaled score level of each pathway. The columns showed each sample, while the rows showed each pathway

differentially expressed genes (Fig. 1C), with upregulation of angiogenesis-related genes in UCMSCs, particularly EGF and HGF and downregulation of IGF-1, a cardio-protective factor in ADMSCs. The biological functions of these DEGs were further analyzed using Gene Ontology (GO) significant pathway enrichment analysis, suggesting that differentially expressed genes were enriched in angiogenesis-related and anti-apoptosis-related pathways

(Fig. 1D). To characterize the difference of functions between UCMSCs and ADMSCs, we calculated the score for pathway related to apoptotic process (Fig. 1E), showing that the apoptotic pathway was downregulated in ADMSCs. These results indicated that UCMSCs and ADMSCs had different gene expression profiles.

UCMSCs had stronger pro-angiogenic capability compared with ADMSCs

In this study, we aimed to identify a more suitable type of MSCs with stronger pro-angiogenic potential for MI repair. Transcriptome analysis revealed differential expression of angiogenesis-related genes between UCMSCs and ADMSCs, such as EGF and HGF (Fig. 1C). Thus, we first examined the pro-angiogenic capacity of UCMSCs and ADMSCs through tube formation assay in vitro. The results showed that both UCMSCs and ADMSCs promoted endothelial cell tube formation compared to controls, showing increased total tube-length, nodes, and junctions. Notably, the ADMSCs group exhibited non-significant trends in node and junction counts (Fig. 2A-D). The in vivo pro-angiogenic capacity of UCMSCs and ADMSCs was further assessed using a Matrigel plug assay in nude mice. The Matrigel plugs contained MSCs transplants had a red gross appearance after transplanting for 14 days (Fig. 2E), indicating significant neovascularization compared with Matrigel plugs without MSCs. CD31 was a marker of blood vessels and the number of CD31-positive cells in Matrigel plugs containing MSCs was significantly higher than that in the control group without MSCs (Fig. 2F, G). Consistent with the in vitro results, UCMSCs were more potent than ADMSCs in inducing the ingrowth of new blood vessels into the Matrigel plugs (Fig. 2F, G). In addition, their pro-angiogenic potentials were compared using an ex vivo aortic ring assay. Quantitative evaluation demonstrated that conditioned medium from both cell types enhanced endothelial sprout formation compared to controls. Notably, conditioned medium from UCMSCs induced more sprouts than ADMSCs-conditioned medium, whereas control groups exhibited minimal sprouting with sporadic cellular outgrowths (Fig. 2H, I).

Furthermore, we examined the mRNA levels of four major pro-angiogenic growth factors and a cardioprotective factor, IGF-1. The mRNA levels on pro-angiogenic factors of bFGF, EGF, HGF, VEGF were elevated in UCMSCs compared to ADMSCs, with bFGF showing only a slight increase (Fig. 2J). These results suggest that UCMSCs and ADMSCs have distinct tissue heterogeneity and that UCMSCs possess greater angiogenic potential than ADMSCs.

ADMSCs had superior therapeutic efficacy of acute MI

Next, we investigated whether UCMSCs, with stronger pro-angiogenic capacity, could possess superior therapeutic efficacy for MI post-transplantation compared with ADMSCs in mice. We established an acute mouse MI model and injected UCMSCs and ADMSCs into the MI border zone immediately after surgery. Echocardiography was performed on day 28 post MSCs transplantation to evaluate heart function recovery in all experiment

mice, excluding one mouse that died in the MI group. Compared with the sham group, the left ventricle ejection fraction (LVEF) and fraction shortening (LVFS) of mice were significantly lower in the MI group (Fig. 3A, B). However, both the UCMSCs and ADMSCs transplantation groups showed improvements in LVEF and LVFS compared with the MI group (Fig. 3A, B). Surprisingly, the ADMSCs transplantation group had better recovery of LVEF and LVFS than UCMSCs transplantation group (Fig. 3A, B). Additionally, we assessed the scar area with Masson's trichrome on day 28 post surgery and cell transplantation (Fig. 3C). Consistent with the recovery of cardiac function, both the UCMSCs and ADMSCs treatment groups had smaller scar size compared with MI group at ~1 mm below the LAD ligation site (Fig. 3D). Notably, the reduction in scar size was more pronounced in ADMSCs group than in UCMSCs group, as shown by the blue area representing fibrotic myocardium in the infarcted heart (Fig. 3C). Together, these results demonstrated that ADMSCs promoted superior cardiac function recovery and limited adverse cardiac tissue remodeling in acute MI compared with UCMSCs.

UCMSCs superiorly augmented angiogenesis in cardiac infarction tissues post acute MI

To elucidate the mechanism underlying the improved cardiac function conferred by MSCs therapy in MI hearts, we first investigated neoangiogenesis in cardiac infarction tissues using blood vessel marker antibodies against CD31 and α-SMA to stain capillaries and arteriole, respectively. On day 28 after MI, both capillary and arteriolar staining densities significantly increased in UCMSCs and ADMSCs treatment groups compared with the MI group (Fig. 4A-D). Notably, the blood vessel staining density was much higher in UCMSCs group than in the ADMSCs group (Fig. 4C, D). Although UCMSCs exhibited superior in vitro pro-angiogenic activity and in vivo neoangiogenesis in the actue MI model, they did not correspondingly outperform ADMSCs in improving cardiac function recovery. This suggests that the enhanced cardiac function recovery mediated by ADMSCs treatment were not attributable to neoangiogenesis after acute MI but rather worked through other mechanisms. Additionally, we traced the fate of transplanted MSCs post transplantation in acute MI. UCMSCs and ADMSCs were labeled with the CM-DiI fluorescent dye (CM-DiI-labeled MSCs) and directly injected into the infarcted mouse hearts to observe their distribution, survival time, and whether transplanted UCMSCs directly differentiated into ECs in the infarcted heart. Results showed that the red fluorescence signal of CM-DiI-labeled MSCs along with green autofluorescence from cardiomyocytes and DAPI - stained nuclei was similarly distributed in the border and infarct zones of hearts treated with UCMSCs
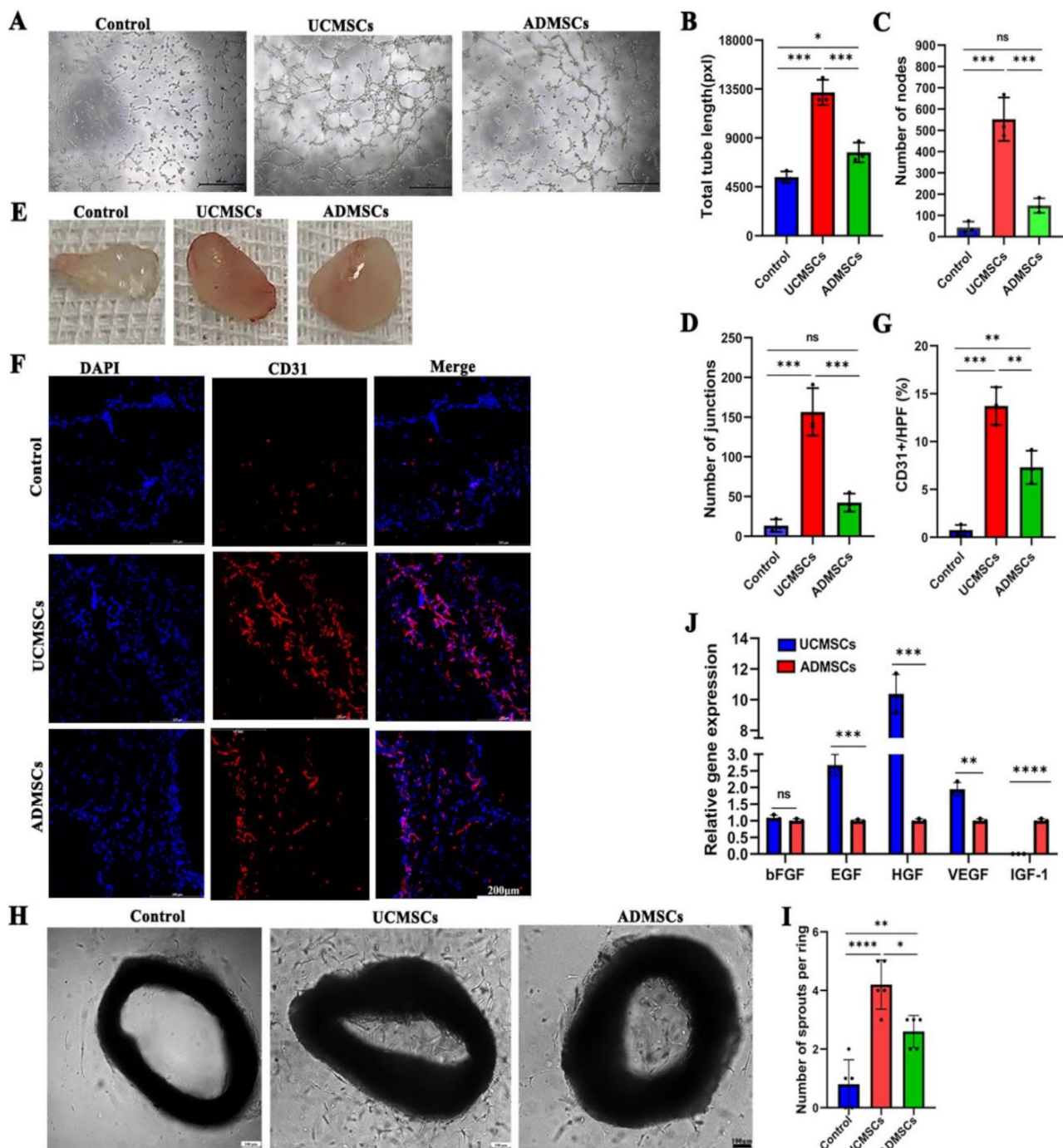
Fig. 2 MSCs stimulated tube formation in vitro and induced neovessel formation in vivo. (**A**) Representative images of tube formation in HUVECs cultured with conditioned medium of UCMSCs or ADMSCs. Scale bar: 500 μm. (**B-D**) Quantification for tube formation assay: total tube length, number of nodes and junctions. n = 3 independent experiments. Data were analyzed using one-way ANOVA. Data are mean ± SD. (**E**) Appearance of Matrigel plug after transplanting MSCs for 14 days in nude mice. (**F**, **G**) Representative images of neovasculature formed by MSCs in Matrigel plugs in nude mice using immunofluorescence staining with anti-CD31 and their quantification. (*n* = 3 Matrigel plugs per group). Scale bar: 200 μm. (**H**, **I**) Representative images of microvessel outgrowth from aortic rings on day 10 cultured in conditioned medium from UCMSCs or ADMSCs, with corresponding number of sprouts. *n* = 5, repeating three times. Scale bar: 100 μm. (**J**) mRNA expression analysis of the paracrine factors bFGF, EGF, HGF, VEGF and IGF-1 in UCMSCs and ADMSCs. *n* = 3 independent experiments. Statistical comparisons were conducted using one-way ANOVA for three groups, and unpaired t test for two-group comparisons. Data are mean ± SD. ns ($p \geq 0.05$), *$p < 0.05$, **$p < 0.01$, ***$p < 0.001$, ****$p < 0.0001$
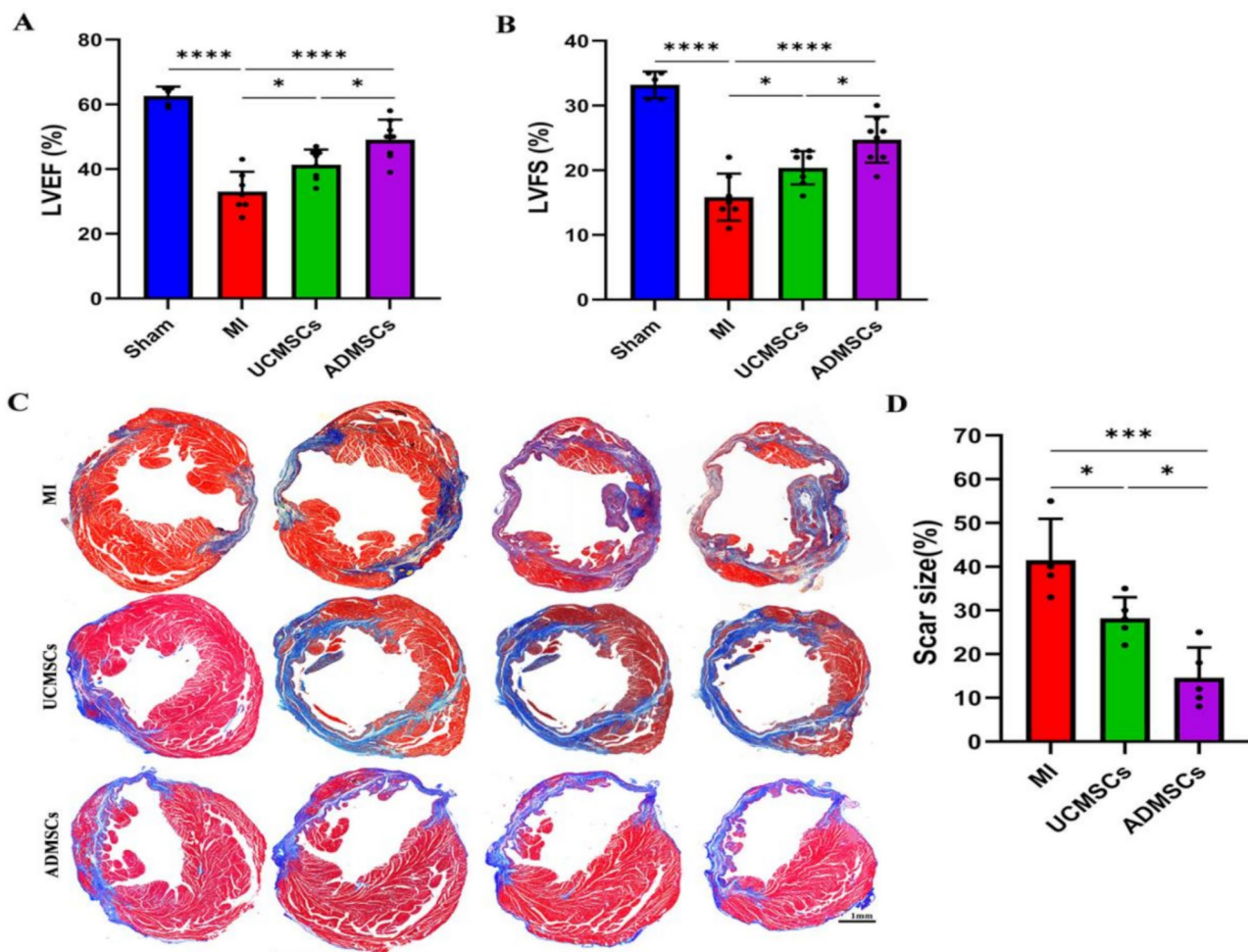
Fig. 3 ADMSCs superiorly improved cardiac function and reduced scar size on day 28 post MI. (**A**, **B**) Intramyocardium injection of UCMSCs and ADMSCs significantly improved LVFS and LVEF after acute MI. $n=5$ in sham, $n=7$ in MI, $n=8$ in UCMSCs and ADMSCs, respectively. (**C**) Representative masson's trichrome staining of cardiac tissues. Scale bar: 1 mm. (**D**) quantification of scar size in each group. $n=4$ in MI, $n=5$ in UCMSCs and ADMSCs, respectively. Statistical comparisons were conducted using one-way ANOVA. Data are mean±SD. *$p < 0.05$, ***$p < 0.001$, ****$p < 0.0001$

and ADMSCs, respectively, and gradually decreased on day 14 after injection (Fig. 4E, F). Immunofluorescence staining showed that although CM-DiI-positive cells could be seen in the infarcted heart for 14 days, no co-localization was observed between CM-DiI-labeled MSCs and a-SMA antibody double staining (Fig. 4G). These results suggest that the transplanted MSCs enhanced new blood vessel formation through paracrine mechanisms rather than via direct differentiation into ECs, which is consistent with the pro-angiogenic gene expression profile detected by qRT-PCR.

ADMSCs protected cardiomyocytes from apoptosis after ischemic injury

In addition to neovascularization, the survival of residual cardiomyocytes is another crucial factor affecting cardiac functional recovery after MI. Since the loss of cardiomyocytes significantly worsens cardiac function.

We evaluated myocardial apoptosis by TUNEL staining in the border zones of hearts on day 1 and day 7 post-MI. The results showed a higher percentage of apoptosis in the boarder zones of the MI group, whereas apoptosis was reduced in groups treated with UCMSCs or ADMSCs at both time points (Fig. 5A-D). Importantly, ADMSCs treatment dramatically attenuated apoptosis in comparison with UCMSCs treatment at the indicated time points (Fig. 5A-D). Given the inhibitory effect of MSCs treatment on myocardial apoptosis, as detected by TUNEL, we further examined the expression of pro-apoptosis related protein Caspase3 and Bax in infarcted hearts via western blotting. The results indicated that Cleaved-caspase3, the active form of Caspase3, and Bax were significantly upregulated in infarcted hearts after MI (Fig. 5E-G). Both UCMSCs and ADMSCs treatments significantly suppressed the expressions of Cleaved-caspase3 and Bax. We further validated the anti-apoptotic
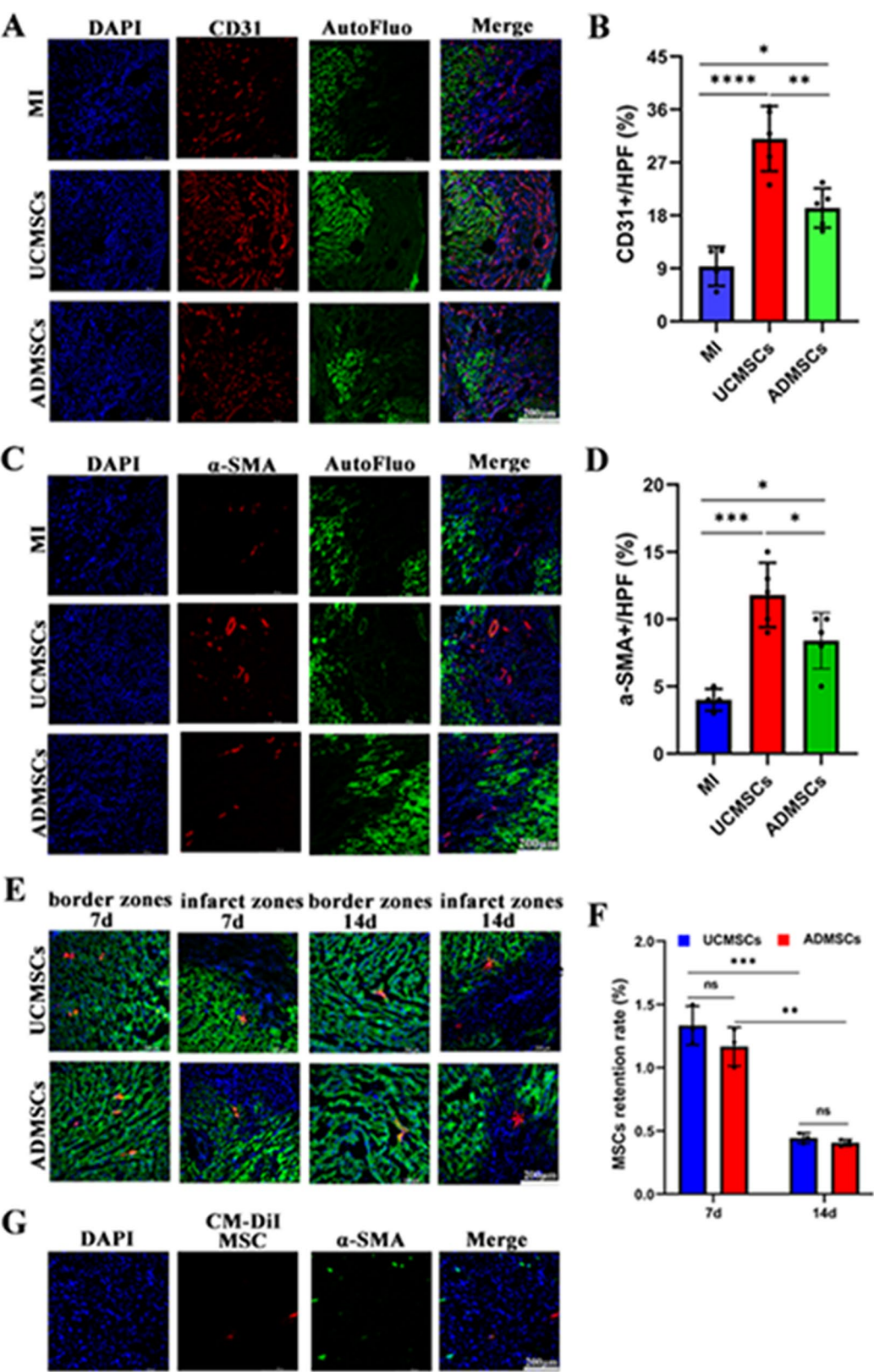
Fig. 4 (See legend on next page.)

(See figure on previous page.)

Fig. 4 UCMSCs transplant superiorly augmented neovascularization in mouse model for MI. (**A**, **C**) Representative images of CD31 and α-SMA staining of heart tissue from mice with MI that received transplantation of saline, UCMSCs or ADMSCs. Scale bar: 200 μm. (**B**, **D**) Quantitative analysis of CD31 and α-SMA density in heart tissue from the different groups on day 28 after surgery and treatment. $n = 4$ in MI, $n = 5$ in UCMSCs and ADMSCs, respectively. Scale bar: 200 μm. (**E**, **F**) Representative images of CM-Dil-labeled MSCs (Red) in border zones and infarct zones and their quantification on day 7 and day 14 post-MI. $n = 3$ per group. Scale bar: 200 μm. (**G**) Representative images of CM-Dil-labeled MSCs and a-SMA double staining on day 14 post-MI. Scale bar: 200 μm. Statistical comparisons were conducted using one-way ANOVA for three groups, and unpaired t test for two-group comparisons. Data are mean ± SD. *$p < 0.05$, **$p < 0.01$, ***$p < 0.001$, ****$p < 0.0001$. AutoFluo (green) indicates auto fluorescence of cardiomyocytes in heart section. ns indicates non-statistical significance

effects of UCMSCs and ADMSCs on H9C2 cardiomyoblasts and HL-1 mouse atrial cardiomyocytes after hypoxia stimulation in vitro by flow cytometric analysis. After 3 h of hypoxia, the apoptosis rate of H9C2 and HL-1 cells was increased compared with normoxic controls. Both of UCMSCs and ADMSCs treatment reduced the hypoxia-induced apoptosis, with ADMSCs superior than UCMSCs (Fig. 5H-J). These observations suggest that ADMSCs exerted a better cardioprotective effects by inhibiting cardiomyocyte apoptosis, which may explain their enhanced promotion of cardiac functional recovery and reduced scar size in acute MI.

Discussion

Angiogenesis is vital for promoting reperfusion and functional recovery of ischemic hearts by restoring blood supply. Consequently, the induction of cardiac angiogenesis has become a key therapeutic strategy for MI [1–3]. Over the past decades, various MSCs from different sources have shown promise in treating MI among preclinical and clinical studies, with potential therapeutic efficacy of MSCs via pro-angiogenic, anti-apoptotic, and anti-inflammatory mechanisms. In particular, pro-angiogenesis has emerged as a new opportunity to be utilized in ischemic heart disease [33–37]. While the ideal origin of MSCs due to their intrinsic heterogeneity still needs to be determined and the predominate mechanism through which MSCs present beneficial effects on MI model are not completely elucidated. In this study, transcriptome sequencing revealed differential gene expression profiles in UCMSCs and ADMSCs. Both types of MSCs demonstrated effective outcomes in improving myocardial function in mouse MI models. Notably, While UCMSCs showed greater pro-angiogenic potential, ADMSCs provided better cardioprotection by inhibiting cardiomyocyte apoptosis. Furthermore, transcriptomic sequencing revealed that ADMSCs downregulated apoptosis-related signaling pathways, and exhibited higher expression levels of cardioprotective factors with anti-apoptotic effects, such as IGF-1, compared to UCMSCs. These findings provided new insights into acute MI therapy and we could take the advantage of MSCs' tissue heterogeneity to screen out optimal cells, such as ADMSCs, for clinical applications.

Compelling evidences indicated that despite meeting a minimal criterion to define MSCs issued by International Society for Cellular Therapy (ISCT) as being plastic adherent, multilineage differentiation, and surface marker expression [38], MSCs isolated from different tissues exhibited distinct properties in surface marker expression profiles, differentiation potential, and transcriptomic/proteomic profiles, which may influence their clinical application [20, 39–43]. Taking all these factors into consideration, we conducted transcriptomic analyses and found differential gene expression in apoptosis-related pathways between UCMSCs and ADMSCs. Functional assays confirmed that UCMSCs had stronger in vitro and in vivo pro-angiogenic capacity than ADMSCs. Therefore, indeed UCMSCs and ADMSCs had obvious tissue heterogeneity. Previous studies documented that bone marrow-derived MSCs (BMSCs) were inclined to differentiate into osteoblasts, whereas UCMSCs inclined to angiogenesis, supporting the concept of 'tissue imprinting' [21, 38, 44]. This heterogeneity of MSCs may influence their clinical applications and result in different functional outcomes. In this study, we applied UCMSCs and ADMSCs to mouse MI models to compare their therapeutic efficacy and explored the underlying mechanics by which MSCs improved cardiac injury and laid the foundation for selecting the best source for cell-based therapy in MI.

Acute and persistent ischemia and hypoxia in the coronary arteries caused by reduced blood flow in acute MI, leading to myocardial necrosis. The idea of promoting angiogenesis to support survival and function by restoring an adequate supply of oxygen and nutrients is promising for treatment of acute MI, our study showed UCMSCs significantly promoted angiogenesis in vitro and vivo and in mice with heart ischemia compared with ADMSCs. Furthermore, previous studies demonstrated that MSCs had the capacity to differentiate into ECs and SMCs, which formed the foundation of vessels [11, 45]. However, in our study, we failed to observe the differentiation of transplanted MSCs into endothelial cells (ECs) post-MI. Meanwhile, mRNA of pro-angiogenic factors (bFGF, EGF, HGF, and VEGF) expression in UCMSCs and ADMSCs were detected. These findings also suggest that MSCs likely improve neovascularization primarily through paracrine mechanisms rather than cell-lineage transdifferentiation. To our knowledge, this study provides the first relatively comprehensive comparison of angiogenic potential between UCMSCs and ADMSCs,
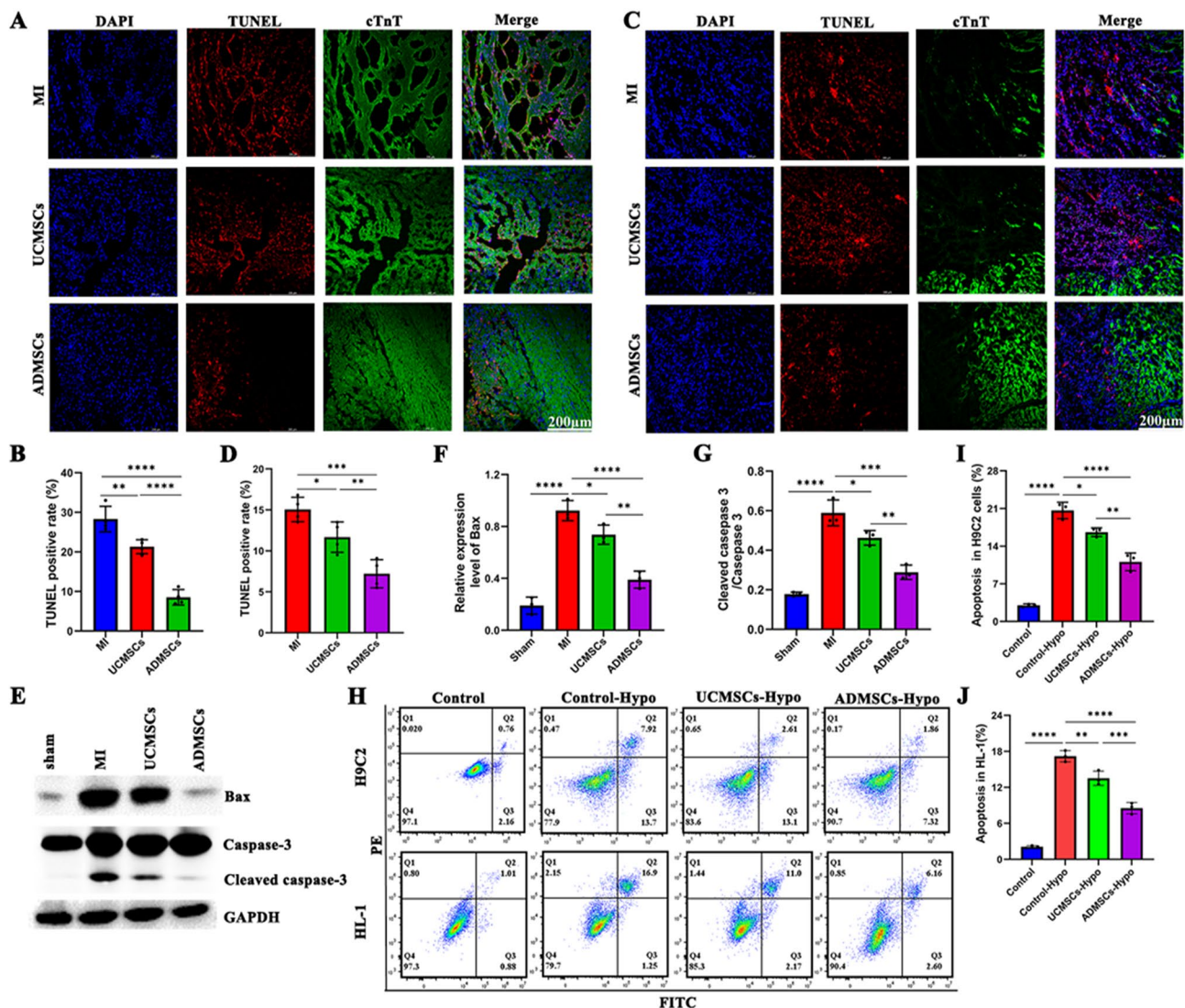
Fig. 5 ADMSCs had better protective effect against apoptosis in myocardial tissues and in hypoxia H9C2 and HL-1cells. (**A**, **C**) Representative images of apoptotic cells on day 1 and day 7 after MI by TUNEL (red) staining. Scale bar: 200 μm. (**B**) Quantitative analysis of apoptotic cells in heart tissue on day 1 from different groups. $n = 4$ per group. (**D**) Quantitative analysis of apoptotic cells in heart tissue on day 7 from different groups. $n = 4$ per group. (**E-G**) The protein expressions of Bax and Cleaved caspase-3 and their quantitation in myocardial tissues on day 28 after surgery and treatment by western blotting. (**H-J**) Apoptosis of H9C2 and HL-1 cells after hypoxia treatment measured by FITC-annexin V/PI double staining analysis using flow cytometry and their qualification from different groups. Statistical comparisons were conducted using one-way ANOVA for three groups, and unpaired t test for two-group comparisons. Data are mean±SD. *$p < 0.05$, **$p < 0.01$, ****$p < 0.0001$. Images of unedited full blots are presented in Supplementary Figure S1

revealing that UCMSCs exhibit superior pro-angiogenic capacity. Similarly, Bian et al. [46] also demonstrated a varying paracrine action in MSCs. According to our hypothesis, UCMSCs with stronger pro-angiogenic capacity should outperform ADMSCs in cardiac function recovery and injured tissue remodeling by facilitating neovascularization at the infarction site. Unexpectedly, although both UCMSCs and ADMSCs improved cardiac function recovery, as indicated by increased LVEF and LVFS, as well as reduced scar size, ADMSCs exhibited superior cardiac functional recovery to UCMSCs. These results clearly suggest that the formation of new

blood vessels following ischemic injury was not the most crucial factor for myocardial repair in acute MI. Thus, in MSCs-based therapy for acute MI, there must be another, more predominant mechanism beyond neovascularization through which ADMSCs achieve superior cardiac functional recovery.

In the hostile ischemic microenvironment during MI, most cardiac cells, including cardiomyocytes, endothelial cells and macrophages, undergo apoptosis. Apoptosis began in infarcted hearts within 3 h, reaching its maximum value at 1–2 days, and was still apparent on day 10 after myocardial infarction [47]. According to previous

results that MSCs prevented ventricular remodeling and restored cardiac function within 72 h [48], the extent of cardiomyocyte loss in the early stages of MI directly correlated with subsequent cardiac dysfunction. Dead cardiomyocytes are subsequently replaced by fibroblasts, leading to ventricular remodeling, wall thinning, scar formation, and ultimately heart failure. Several studies have demonstrated that inhibition of cardiomyocyte apoptosis results in reduced infarct size after MI. Therefore, cardiomyocyte apoptosis significantly contributes to adverse cardiac remodeling and subsequent cardiac dysfunction post-AMI [49–52]. Therefore, diminution of cardiomyocyte apoptosis was of extreme importance for cardiac functional recovery, which were extensively explored both in vitro and in vivo studies in treating ischemia-induced heart injury [53–57]. Apoptosis could be assessed by some indicators, such as TUNEL staining and Caspase-3 detection. Studies have indicated that the Caspase family was the promoter and executioner of apoptosis in mammals, among which Caspase-3 was the most critical downstream apoptotic protease. Bax, a pro-apoptotic protein, promoted apoptosis by activating Caspase-3. In this study, we found that both UCMSCs and ADMSCs reduced the apoptosis rate and decreased levels of apoptosis-related protein such as cleaved Caspase-3 and Bax in infarcted tissue after acute MI. Notably, ADMSCs exhibited better anti-apoptotic effects compared with UCMSCs in infarcted heart, which was further confirmed in H9C2 and HL-1 cells under hypoxic conditions.

These findings, along with the improvements in LVFS and LVEF and the reduction in scar size, confirmed that ADMSCs protected the heart against MI injury mainly through inhibiting apoptosis in residual cells. Since apoptosis accounted for 86% of total cardiomyocytes loss and was the major determinant of infarct size, therapies that able to limit myocardial infarct size can alleviate cardiac dysfunction and inhibit the development of adverse myocardial remodeling [57]. Notably, transcriptome sequencing analysis and our mRNA quantification reveals that ADMSCs exhibit higher expression levels of IGF-1, a potent cardioprotective cytokine known to mediate anti-apoptotic effects. Thus, we concluded that protecting residual cells played a more prominent role than vascular regeneration or angiogenesis in MSCs-based therapy after acute MI. Collectively, our results suggest that ADMSCs are more suitable than UCMSCs for treating acute MI in mice, holding great potential for clinical research.

There are still some limitations in current study. First, this study only investigated acute MI model and concluded that anti-apoptosis of residual cells was more crucial than neovascularization in MSCs-based therapy. We did not compare the therapeutic efficacy of UCMSCs and ADMSCs in chronic MI models. Second, the exact mechanism by which UCMSCs and ADMSCs had superior neovascularization and anti-apoptosis, respectively, remained to be elucidated. Third, only UCMSCs and ADMSCs were examined in this study. There are also kinds of MSCs derived from many other adult tissues, such as bone marrow, peripheral blood, dental pulp, placenta, and endometrial tissues etc. To select the best suitable cells for the therapy of MI, more candidate MSCs should be included.

Conclusions

In this study, we applied two kinds of MSCs with different angiogenic potential and anti-apoptosis to compare their cardiac function recovery in therapy of acute MI. Results showed survival protection of residual cells played a more prominent role than angiogenesis in cardiac repair after acute MI in MSCs-based therapy. Our study provided new insight into therapeutic strategy of acute MI and we could screen the optimal type of MSCs based on their tissue heterogeneity for superior clinical applications in acute MI.

Abbreviations

α-SMA	Alpha-smooth muscle actin
bFGF	Basic fibroblast growth factor
VEGF	Vascular endothelial growth factor
EGF	Epidermal growth factor
HGF	Hepatocyte growth factor
IGF-1	Insulin-like growth factor-1

Supplementary Information

The online version contains supplementary material available at https://doi.org/10.1186/s13287-025-04378-3.

Supplementary Material 1

Data availability
The raw data underpinning the conclusions of this paper will be provided by the authors to any qualified researcher without undue reservation. The raw sequence data reported in this paper have been deposited in the Genome Sequence Archive (Genomics, Proteomics & Bioinformatics 2021) in National Genomics Data Center (Nucleic Acids Res 2024), China National Center for Bioinformation / Beijing Institute of Genomics, Chinese Academy of Sciences (GSA-Human: HRA009484) that are publicly accessible at https://ngdc.cncb.ac.cn/gsa-human.

Pan *et al. Stem Cell Research & Therapy*   (2025) 16:236

Page 14 of 15

Declarations

Ethics approval and consent to participate
All animal experiments were performed in compliance with the guidelines and regulations from the animal experimentation committee of Nanjing Medical University (Ethics Committee of Nanjing First Hospital). (Project title: To compare the protection of MSC derived from different sources against myocardial infarction; Approval No. DWSY-22115244; Date of approval: 2022-8-25). All procedures involving human-derived materials were granted by the Medical Ethics Committees of Nanjing Drum Tower Hospital, The Affiliated Hospital of Nanjing University Medical School. (Project title: Utilization of Clinical Patient Samples (Tissue/Blood/Body Fluids) and Aborted Fetal Tissue to Extract Stem Cells for Basic and Clinical Research in Regenerative Medicine and Treatment of Clinical Diseases; Approval No.2017-161-01; Date of approval: 2017-12-26). All participants provided written informed consent for participation in the study.

Consent for publication
Not applicable.

Competing interests
The authors declare that they have no competing interests.

Author details
[1]Clinical Medicine Research Center, Nanjing Drum Tower Hospital, The Affiliated Hospital of Nanjing University Medical School, Nanjing, Jiangsu Province, China
[2]The Department of Thoracic and Cardiovascular Surgery, Nanjing First Hospital, Nanjing Medical University, Nanjing, Jiangsu Province, China
[3]Clinical Stem Cell Center, Nanjing Drum Tower Hospital, Clinical Medical College of Traditional Chinese and Western Medicine, Nanjing University of Chinese Medicine, Nanjing, Jiangsu Province, China
[4]Clinical Stem Cell Center, the Affiliated Drum Tower Hospital of Nanjing University Medical School, Nanjing, Jiangsu Province, China

References
1. Badimon L, Borrell M. Microvasculature recovery by angiogenesis after myocardial infarction. Curr Pharm Des. 2018;24:2967–73.
2. Barrere-Lemaire S, Vincent A, Jorgensen C, Piot C, Nargeot J, Djouad F. Mesenchymal stromal cells for improvement of cardiac function following acute myocardial infarction: a matter of timing. Physiol Rev. 2024;104:659–725.
3. Malektaj H, Nour S, Imani R, Siadati MH. Angiogenesis induction as a key step in cardiac tissue regeneration: from angiogenic agents to biomaterials. Int J Pharm. 2023;643:123233.
4. Zhang LL, Xiong YY, Yang YJ. The vital roles of mesenchymal stem cells and the derived extracellular vesicles in promoting angiogenesis after acute myocardial infarction. Stem Cells Dev. 2021;30:561–77.
5. Huang P, Wang L, Li Q, Xu J, Xu J, Xiong Y, Chen G, Qian H, Jin C, Yu Y et al. Combinatorial treatment of acute myocardial infarction using stem cells and their derived exosomes resulted in improved heart performance. Stem Cell Res Ther. 2019;10.
6. Vrijsen KR, Maring JA, Chamuleau SAJ, Verhage V, Mol EA, Deddens JC, Metz CHG, Lodder K, van Eeuwijk ECM, van Dommelen SM, et al. Exosomes from cardiomyocyte progenitor cells and mesenchymal stem cells stimulate angiogenesis via EMMPRIN. Adv Healthc Mater. 2016;5:2555–65.
7. Byrne RA, Rossello X, Coughlan JJ, Barbato E, Berry C, Chieffo A, Claeys MJ, Dan GA, Dweck MR, Galbraith M, et al. 2023 ESC guidelines for the management of acute coronary syndromes. Eur Heart J. 2023;44:3720–26.
8. Poomani MS, Mariappan I, Perumal R, Regurajan R, Muthan K, Subramanian V. Mesenchymal stem cell (MSCs) therapy for ischemic heart disease: A promising frontier. Glob Heart. 2022;17:19.
9. Lim M, Wang W, Liang L, Han ZB, Li Z, Geng J, Zhao M, Jia H, Feng J, Wei Z, et al. Intravenous injection of allogeneic umbilical cord-derived multipotent mesenchymal stromal cells reduces the infarct area and ameliorates cardiac function in a Porcine model of acute myocardial infarction. Stem Cell Res Ther. 2018;9:129.
10. Silva GV, Litovsky S, Assad JA, Sousa AL, Martin BJ, Vela D, Coulter SC, Lin J, Ober J, Vaughn WK, et al. Mesenchymal stem cells differentiate into an endothelial phenotype, enhance vascular density, and improve heart function in a canine chronic ischemia model. Circulation. 2005;111:150–56.
11. Zhang C, Lin Y, Liu Q, He J, Xiang P, Wang D, Hu X, Chen J, Zhu W, Yu H. Growth differentiation factor 11 promotes differentiation of MSCs into endothelial-like cells for angiogenesis. J Cell Mol Med. 2020;24:8703–17.
12. Liu CB, Huang H, Sun P, Ma SZ, Liu AH, Xue J, Fu JH, Liang YQ, Liu B, Wu DY, et al. Human umbilical Cord-Derived mesenchymal stromal cells improve left ventricular function, perfusion, and remodeling in a Porcine model of chronic myocardial ischemia. Stem Cells Transl Med. 2016;5:1004–13.
13. Yang GD, Ma DS, Ma CY, Bai Y. Research progress on cardiac tissue construction of mesenchymal stem cells for myocardial infarction. Curr Stem Cell Res Ther. 2024;19:942–58.
14. Guo Y, Yu Y, Hu S, Chen Y, Shen Z. The therapeutic potential of mesenchymal stem cells for cardiovascular diseases. Cell Death Dis. 2020;11:349.
15. Razeghian-Jahromi I, Matta AG, Canitrot R, Zibaeenezhad MJ, Razmkhah M, Safari A, Nader V, Roncalli J. Surfing the clinical trials of mesenchymal stem cell therapy in ischemic cardiomyopathy. Stem Cell Res Ther. 2021;12:361.
16. He YC, Yuan GD, Li N, Ren MF, Qian Z, Deng KN, Wang LC, Xiao WL, Ma N, Stamm C, et al. Recent advances in mesenchymal stem cell therapy for myocardial infarction. Clin Hemorheol Microcirc. 2024;87:383–98.
17. Moll G, Ankrum JA, Kamhieh-Milz J, Bieback K, Ringdén O, Volk HD, Geissler S, Reinke P. Intravascular mesenchymal stromal/stem cell therapy product diversification: time for new clinical guidelines. Trends Mol Med. 2019;25:149–63.
18. Xu J, Xiong YY, Li Q, Hu MJ, Huang PS, Xu JY, Tian XQ, Jin C, Liu JD, Qian L, et al. Optimization of timing and times for administration of Atorvastatin-Pretreated mesenchymal stem cells in a preclinical model of acute myocardial infarction. Stem Cells Transl Med. 2019;8:1068–83.
19. Li J, Hu S, Zhu D, Huang K, Mei X, Lopez de Juan Abad B, Cheng K. All roads lead to Rome (the Heart): Cell Retention and Outcomes From Various Delivery Routes of Cell Therapy Products to the Heart. J Am Heart Assoc. 2021;10:e020402.
20. Costa LA, Eiro N, Fraile M, Gonzalez LO, Saá J, Garcia-Portabella P, Vega B, Schneider J, Vizoso FJ. Functional heterogeneity of mesenchymal stem cells from natural niches to culture conditions: implications for further clinical uses. Cell Mol Life Sci. 2021;78:447–67.
21. Lobov A, Kuchur P, Khizhina A, Kotova A, Ivashkin A, Kostina D, Klausen P, Khokhlova E, Repkin E, Postnikova K, et al. Mesenchymal cells retain the specificity of embryonal origin during osteogenic differentiation. Stem Cells. 2024;42:76–89.
22. Calcat ICS, Rendra E, Scaccia E, Amadeo F, Hanson V, Wilm B, Murray P, O'Brien T, Taylor A, Bieback K. Harmonised culture procedures minimise but do not eliminate mesenchymal stromal cell donor and tissue variability in a decentralised multicentre manufacturing approach. Stem Cell Res Ther. 2023;14:120.
23. Xie Y, Liu S, Wang L, Yang H, Tai C, Ling L, Chen L, Liu S, Wang B. Individual heterogeneity screened umbilical cord-derived mesenchymal stromal cells with high Treg promotion demonstrate improved recovery of mouse liver fibrosis. Stem Cell Res Ther. 2021;12:359.
24. Ganguly A, Swaminathan G, Garcia-Marques F, Regmi S, Yarani R, Primavera R, Chetty S, Bermudez A, Pitteri SJ, Thakor AS. Integrated transcriptome-proteome analyses of human stem cells reveal source-dependent differences in their regenerative signature. Stem Cell Rep. 2023;18:190–204.
25. Neo SH, Her Z, Othman R, Tee CA, Ong LC, Wang Y, Tan I, Tan J, Yang Y, Yang Z, et al. Expansion of human bone marrow-derived mesenchymal stromal cells with enhanced Immunomodulatory properties. Stem Cell Res Ther. 2023;14:259.
26. Xia X, Sui Y, Zhou J, Li S, Ma X, Jiang J, Yan Y. Augmenting mesenchymal stem cell therapy for osteoarthritis via inflammatory priming: a comparative study on mesenchymal stem cells derived from various perinatal tissue sources. Front Cell Dev Biol. 2023;11:1279574.
27. Jiang L, Yang A, Li X, Liu K, Tan J. Down-regulation of VCAM-1 in bone mesenchymal stem cells reduces inflammatory responses and apoptosis to improve cardiac function in rat with myocardial infarction. Int Immunopharmacol. 2021;101:108180.
28. Xie Y, Liu W, Liu S, Wang L, Mu D, Cui Y, Cui Y, Wang B. The quality evaluation system establishment of mesenchymal stromal cells for cell-based therapy products. Stem Cell Res Ther. 2020;11:176.
29. Gao T, Huang F, Wang W, Xie Y, Wang B. Interleukin-10 genetically modified clinical-grade mesenchymal stromal cells markedly reinforced functional

30. recovery after spinal cord injury via directing alternative activation of macrophages. Cell Mol Biol Lett. 2022;27:27.
30. Wu T, Hu E, Xu S, Chen M, Guo P, Dai Z, Feng T, Zhou L, Tang W, Zhan L, et al. ClusterProfiler 4.0: A universal enrichment tool for interpreting omics data. Innov (Camb). 2021;2:100141.
31. Baker M, Robinson SD, Lechertier T, Barber PR, Tavora B, D'Amico G, Jones DT, Vojnovic B, Hodivala-Dilke K. Use of the mouse aortic ring assay to study angiogenesis. Nat Protoc. 2011;7:89–104.
32. Alfaro MP, Pagni M, Vincent A, Atkinson J, Hill MF, Cates J, Davidson JM, Rottma J, Lee E, Young PP. The Wnt modulator sFRP2 enhances mesenchymal stem cell engraftment, granulation tissue formation and myocardial repair. Proc Natl Acad Sci U S A. 2008;105:18366–71.
33. Zhang J, Li J, Qu X, Liu Y, Harada A, Hua Y, Yoshida N, Ishida M, Tabata A, Sun L, et al. Development of a Thick and functional human adipose-derived stem cell tissue sheet for myocardial infarction repair in rat hearts. Stem Cell Res Ther. 2023;14:380.
34. Yang L, Liu N, Yang Y. Astragaloside IV-induced BMSC exosomes promote neovascularization and protect cardiac function in myocardial infarction mice via the miR-411/HIF-1alpha axis. J Liposome Res. 2024;34:452–63.
35. Sun J, Shen H, Shao L, Teng X, Chen Y, Liu X, Yang Z, Shen Z. HIF-1alpha overexpression in mesenchymal stem cell-derived exosomes mediates cardioprotection in myocardial infarction by enhanced angiogenesis. Stem Cell Res Ther. 2020;11:373.
36. Tao B, Cui M, Wang C, Ma S, Wu F, Yi F, Qin X, Liu J, Wang H, Wang Z, et al. Percutaneous intramyocardial delivery of mesenchymal stem cells induces superior improvement in regional left ventricular function compared with bone marrow mononuclear cells in Porcine myocardial infarcted heart. Theranostics. 2015;5:196–205.
37. Xu CM, Sabe SA, Brinck-Teixeira R, Sabra M, Sellke FW, Abid MR. Visualization of cardiac uptake of bone marrow mesenchymal stem cell-derived extracellular vesicles after intramyocardial or intravenous injection in murine myocardial infarction. Physiol Rep. 2023;11:e15568.
38. Elahi KC, Klein G, Avci-Adali M, Sievert KD, MacNeil S, Aicher WK. Human mesenchymal stromal cells from different sources diverge in their expression of cell surface proteins and display distinct differentiation patterns. Stem Cells Int. 2016;2016:5646384.
39. Chen P, Tang S, Li M, Wang D, Chen C, Qiu Y, Fang Z, Zhang H, Gao H, Weng H, et al. Single-Cell and Spatial transcriptomics decodes Wharton's Jelly-Derived mesenchymal stem cells heterogeneity and a subpopulation with wound repair signatures. Adv Sci (Weinh). 2023;10:e2204786.
40. Panepucci RA, Siufi JL, Silva WA Jr, Proto-Siquiera R, Neder L, Orellana M, Rocha V, Covas DT, Zago MA. Comparison of gene expression of umbilical cord vein and bone marrow-derived mesenchymal stem cells. Stem Cells. 2004;22:1263–78.
41. Chen JY, Mou XZ, Du XC, Xiang C. Comparative analysis of biological characteristics of adult mesenchymal stem cells with different tissue origins. Asian Pac J Trop Med. 2015;8:739–46.
42. Wang ZG, He ZY, Liang S, Yang Q, Cheng P, Chen A. M. Comprehensive proteomic analysis of exosomes derived from human bone marrow, adipose tissue, and umbilical cord mesenchymal stem cells. Stem Cell Res Ther. 2020;11:511.
43. Xu L, Liu Y, Sun Y, Wang B, Xiong Y, Lin W, Wei Q, Wang H, He W, Wang B, et al. Tissue source determines the differentiation potentials of mesenchymal stem cells: a comparative study of human mesenchymal stem cells from bone marrow and adipose tissue. Stem Cell Res Ther. 2017;8:275.
44. Burja B, Barlic A, Erman A, Mrak-Poljsak K, Tomsic M, Sodin-Semrl S, Lakota K. Human mesenchymal stromal cells from different tissues exhibit unique responses to different inflammatory stimuli. Curr Res Transl Med. 2020;68:217–24.
45. Shi W, Xin Q, Yuan R, Yuan Y, Cong W, Chen K. Neovascularization: the main mechanism of MSCs in ischemic heart disease therapy. Front Cardiovasc Med. 2021;8:633300.
46. Bian D, Wu Y, Song G, Azizi R, Zamani A. The application of mesenchymal stromal cells (MSCs) and their derivative exosome in skin wound healing: a comprehensive review. Stem Cell Res Ther. 2022;13:24.
47. Olivetti G, Quaini F, Sala R, Lagrasta C, Corradi D, Bonacina E, Gambert SR, Cigola E, Anversa P. Acute myocardial infarction in humans is associated with activation of programmed myocyte cell death in the surviving portion of the heart. J Mol Cell Cardiol. 1996;28:2005–16.
48. Gnecchi M, He H, Liang OD, Melo LG, Morello F, Mu H, Noiseux N, Zhang L, Pratt RE, Ingwall JS, et al. Paracrine action accounts for marked protection of ischemic heart by Akt-modified mesenchymal stem cells. Nat Med. 2005;11:367–68.
49. Chen QS, Zheng AC, Xu XL, Shi ZN, Yang M, Sun SS, Wang LY, Wang YM, Zhao HG, Xiao QZ, et al. Nrf3-Mediated mitochondrial superoxide promotes cardiomyocyte apoptosis and impairs cardiac functions by suppressing Pitx2. Circulation. 2025;151:1024–46.
50. Chen YF, Shan SY, Xue QQ, Ren Y, Wu QH, Chen JW, Yang K, Cao JM. Sirtuin1 mitigates hypoxia-induced cardiomyocyte apoptosis in myocardial infarction via PHD3/HIF-1α. Mol Med. 2025;31:100.
51. He YR, Pang S, Huang J, Zhu K, Tong JY, Tang YL, Ma GS, Chen LJ. Blockade of RBP-J-Mediated Notch signaling pathway exacerbates cardiac remodeling after infarction by increasing apoptosis in mice. Biomed Res Int. 2018;2018:5207031.
52. Li NN, Xia N, He JY, Liu ML, Gu MY, Lu YZ, Yang HY, Hao ZH, Zha LF, Wang XH, et al. Amphiregulin improves ventricular remodeling after myocardial infarction by modulating autophagy and apoptosis. FASEB J. 2024;38:e23488.
53. Tripathi H, Domingues A, Donahue R, Cras A, Guerin CL, Gao E, Levitan B, Ratajcza MZ, Smadja DM, Abdel-Latif A, et al. Combined transplantation of human MSCs and ECFCs improves cardiac function and decrease cardiomyocyte apoptosis after acute myocardial infarction. Stem Cell Rev Rep. 2023;19:573–77.
54. Xu H, Wang Z, Liu L, Zhang B, Li B. Exosomes derived from adipose tissue, bone marrow, and umbilical cord blood for cardioprotection after myocardial infarction. J Cell Biochem. 2020;121:2089–102.
55. Mishra PK, Adameova A, Hill JA, Baines CP, Kang PM, Downey JM, Narula J, Takahashi M, Abbate A, Piristine HC, et al. Guidelines for evaluating myocardial cell death. Am J Physiol Heart Circ Physiol. 2019;317:H891–922.
56. Peng Y, Zhao JL, Peng ZY, Xu WF, Yu GL. Exosomal miR-25-3p from mesenchymal stem cells alleviates myocardial infarction by targeting pro-apoptotic proteins and EZH2. Cell Death Dis. 2020;11:317.
57. Anversa P, Cheng W, Liu Y, Leri A, Redaelli G, Kajstura J. Apoptosis and myocardial infarction. Basic Res Cardiol. 1998;93(Suppl 3):8–12.

Publisher's note